



PERIODIC METAFFOUNDATIONS FOR THE PROTECTION OF STORAGE TANKS AGAINST HORIZONTAL GROUND ACCELERATIONS

O. S. Bursi (1) , M. Wenzel (2) , R. Andreotti (3) , I. Antoniadis (4)

(1) Full Professor, Department of Civ., Env. and Mech. Engineering, University of Trento, Trento, ITALY, oreste.bursi@unitn.it

(2) PhD Student, Department of Civ., Env. and Mech. Engineering, University of Trento, Trento, ITALY, moritz.wenzel@unitn.it

(3) PhD Student Department of Civ., Env. and Mech. Engineering, University of Trento, Trento, ITALY, roberto.andreotti@unitn.it

(4) Full Professor, Department of Mech. Eng., National Technical University of Athens, Athens, GREECE, antogian@central.ntua.gr

Abstract

This paper introduces a novel seismic isolation system based on metamaterial concepts for the reduction of ground motion-induced vibrations in fuel storage tanks. Herein, we propose two finite locally resonant Metafoundation for large fuel storage tanks: i) a foundation equipped with nonlinear hysteretic dampers; and ii) a foundation equipped with negative stiffness devices. Both are optimized considering the stochastic nature of ground motion, modelled with a modified Kanai-Tajimi filter in the stationary frequency domain, and the superstructure, chosen to be a fuel storage tank. For the first type of metafoundation, we optimize the non-linear behavior of damper devices employing a Bouc-Wen hysteretic model. In particular, we reduce the non-linear differential equations of Bouc-Wen models to a system of linear equations through the stochastic linearization technique. The optimal values for these coefficients can then be found with an established optimization procedure. Finally, we test the optimized systems against natural seismic records with non-linear time history analyses. Nonetheless, one of their main drawbacks to date, is the excessive size of the necessary resonators and, consequently, the uneconomic design they require. In order to tackle this problem, we also apply the concept of negative stiffness to a metamaterial-based foundation system and analyze the potential improvements such a mechanism may have on the metamaterial as well as the coupled structural behavior. Negative stiffness is a property that cannot be achieved through conventional measures. Therefore, a particular device will be designed, which can be implemented into the metamaterial-based structure. The inevitable non-linearity of such a mechanism will be discussed and taken into account herein, while the advantages of the negative stiffness element (NSE) will be highlighted. Additionally, through an optimization in the frequency domain and non-linear time history analyses (THAs), the performance of the system coupled with a fuel storage tank will be elaborated.

Keywords: seismic risk mitigation; industrial facilities; slender tank; finite-lattice metamaterials; attenuation zones.



1. Introduction

Earthquakes represent a significant hazard for the safety and integrity of crucial infrastructures, such as fuel storage tanks of industrial installations, which have proven to be particularly vulnerable, as demonstrated by past seismic events ([1], [2]). Typical seismic isolation system such as rubber bearings [3] and concave sliding bearings [4] can impose significant horizontal displacements, that can induce damages to critical pipeline components such as elbows and joints. Therefore, within the field of metamaterials, this work is dedicated to the development of a metamaterial-based foundation endowed with different nonlinear devices devoted to increase structural damping and reduce the structural stiffness.

Relatively to the former, the selection of proper dampers, [6], suggested to use wire ropes, which provide good isolation properties and high dissipative capabilities. As a result, these devices can achieve equivalent damping ratios of 15-20 percent associated with favorable production and maintenance costs. In view of optimization, here the cyclic behavior of wire ropes is reproduced with a hysteretic Bouc-Wen model [7].

The aforementioned system design was proposed by [8], who found that the horizontal stiffness of the system plays a vital role for metamaterial based foundations, and subsequently proposed the column design used herein. After further development, [6] then highlighted that common construction standards can be fulfilled, but their restrictions resulted in a foundation height of 4 m, which cannot be regarded as economical. With the herein proposed negative stiffness devices (NSE) we aim to improve the feasibility for seismic metamaterials by amplifying the resonator motion, while simultaneously softening the horizontal stiffness.

In order to achieve the best performance of a Metafoundation, the optimization of both the non-linear components previously presented are pursued hereinafter. The superstructure is represented by a fuel storage tank and its equivalent 1D lumped mass model [9]. Therefore, the objective function is represented by the interstory drift or the absolute acceleration of the impulsive mode of the tank. In order to take into account the stochastic nature of the seismic input, the computations are carried out in the frequency domain and because systems are linear elastic in that domain, a stochastic equivalent linearization technique (SLT) is employed for the Bouc-Wen model [10]. A Kanai-Tajimi filter is used as seismic input. The resulting optimized Metafoundations were then verified through nonlinear time history analyses (THAs). After this, we develop a mechanism that can effectively produce a negative stiffness and subsequently reduce the dimensions of the Metafoundation. The effects of the nonlinearity are taken into account and the complete coupled system (tank + foundation) is investigated under real ground motions.

2. Description of the structure endowed with hysteretic components

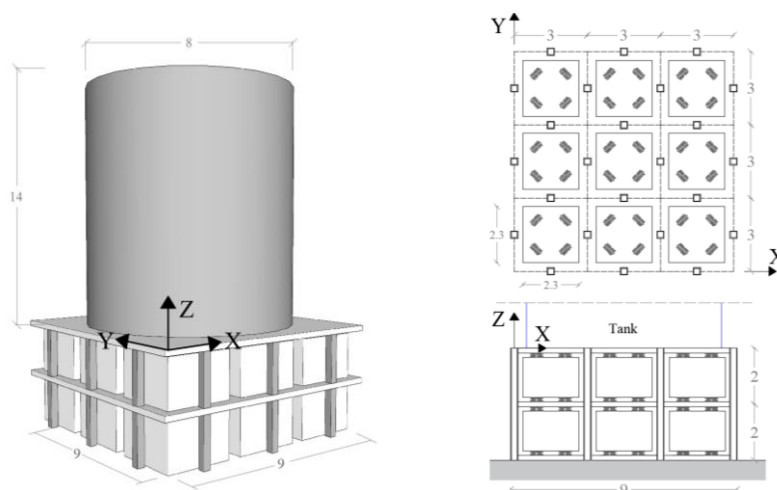


Fig. 1 – Coupled foundation -tank system: isometric view, layout and section.

The Metafoundation is composed of a finite number of unit cells realized with steel columns with hollow sections and concrete slabs, see Fig. 1a. Each unit cell contains a concrete mass, linked to the foundation. The construction site was chosen to be Priolo Gargallo (Italy), which is characterized by a peak ground acceleration



of 0.56g at a return period of 2475 years. The foundation-tank coupled system was designed to remain undamaged even for SSE events, according to the Italian Code (NTC 2008). Two foundations were designed with one and two layers of resonators, as in [6]. The hydrodynamic response of the tank is modeled with the simplified procedure proposed by Malhotra et al. [9], who reduce the tank response to the contribution of the impulsive and convective modes. Furthermore, the concrete resonators are assumed to be suspended by wire ropes, as depicted in Fig 1b and c.

Table 1. Parameters for the 1D tank model according to [9].

m_i [kg]	m_c [kg]	k_i [N/m]	k_c [N/m]	c_i [Ns/m]	c_c [Ns/m]
4,52E+10	8,58E+09	8,35E+13	3,86E+10	1,94E+11	1,82E+08

2.1 Modelling of wire ropes

Since all the resonators of one floor have the same mechanical properties, the coupled system is modelled by condensing the resonators in the same DOF, therefore modelling a Condensed Mass System (CMS). The well-known Bouc-Wen model has been studied extensively in literature to capture the hysteretic behavior of many seismic devices [11]. In this model, the EOM of a single degree of freedom system reads

$$m\ddot{u}(t) + c\dot{u}(t) + R(t) = F(t) \quad (1)$$

where $R(t)$ is the nonlinear restoring force, which can be computed with,

$$R(t) = \alpha k u(t) + (1 - \alpha) k u_y z(t) \quad (2)$$

where k and u_y are the yielding stiffness and displacement, respectively, whereas the dimensionless hysteretic component z is given by the solution of the non-linear differential equation,

$$\dot{z}(t) = u_y^{-1} [A \dot{u}(t) - \gamma |\dot{u}(t)| |z(t)|^{n-1} z(t) - \beta \dot{u}(t) |z(t)|^n] \quad (3)$$

Here A , β , γ , and the exponent n are parameters that control the shape and smoothness of the force-displacement loop. In (2) $\alpha = k_p/k_0$ is the postyielding to preyielding stiffness ratio, with

$$k_0 = \left(\frac{\partial R(u, \dot{u}, z)}{\partial u} \right)_{z=0} = \alpha k + (1 - \alpha) k A \quad k_p = \left(\frac{\partial R(u, \dot{u}, z)}{\partial u} \right)_{z=z_{max}} = \alpha k_0 \quad (4)$$

in which $z_{max} = [A / (\beta + \gamma)]^{1/n}$. By selecting suitable values for the parameters A , β , γ and n , the Bouc-Wen model can yield nonlinearities including hardening or softening. By choosing $n=1$, (3) can easily be solved analytically with simpler exponential functions, as shown by [11]. Fig. 2 shows the linear and nonlinear modeling of the coupled foundation-tank system for two-layered foundation cases.

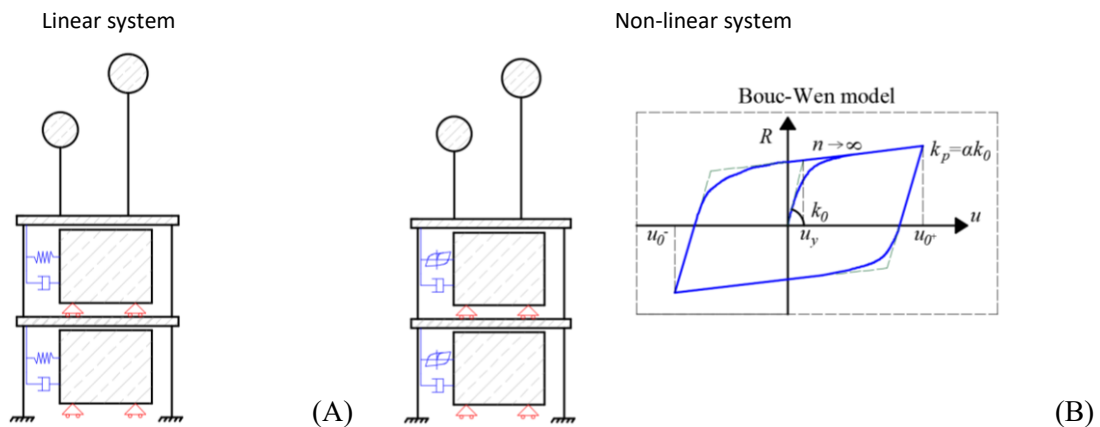


Fig. 2 – Dynamic system of foundation and tank: (A) Linear elastic system; (B) nonlinear system.



2.2 Modelling of seismic input

The seismic input is modelled as a stationary Gaussian filtered white noise random process with zero mean and spectral intensity S_0 . The widely used Kanai-Tajimi filter is adopted here, with a second filter in series proposed by Clough and Penzien to avoid unrealistic filter values in the low-frequency range. For brevity, it is referred to as KTCP filter. The power spectral density function of this filter can be expressed as,

$$S_{\ddot{u}_g}(\omega) = S_0 \frac{4 \zeta_g^2 \omega_g^2 \omega^2 + \omega_g^4}{4 \zeta_g^2 \omega_g^2 \omega^2 + (\omega_g^2 - \omega^2)^2} \frac{\omega^4}{4 \zeta_g^2 \omega_g^2 \omega^2 + (\omega_g^2 - \omega^2)^2} \quad (5)$$

The parameters were chosen to match the ground motion characteristics of a specific construction site, i.e. Priolo Gargallo, at a return period of 2475 years. More precisely, their values amount to $S_0 = 0.09$, $\omega_g = 14$, $\zeta_g = 0.6$, $\omega_f = 0.75$, and $\zeta_f = 1.9$, for this see also Ref. [6].

3. Optimization of the Metafoundation

In order to find the optimal frequency and damping ratio of the resonators, the superstructure as well as the ground motion need to be taken into account. Firstly, we write down the EOMs for a coupled system with,

$$\mathbf{M}\ddot{\mathbf{u}}(t) + \mathbf{C}\dot{\mathbf{u}}(t) + \mathbf{K}\mathbf{u}(t) + \mathbf{R}(t) = \mathbf{F}(t) \quad (6)$$

Here, \mathbf{M} , \mathbf{K} , and \mathbf{C} , represent the mass, stiffness, and damping matrices, while $\mathbf{u}(t)$ denotes the displacement vector and $\mathbf{F}(t)$ contains the external force. Furthermore, $\mathbf{R}(t)$ denotes the nonlinear restoring force deriving from the wire ropes Eq. (2) or, as will be discussed later, the NSE Eq. (26). For both systems the nonlinear term $\mathbf{R}(t)$ will be linearized and represented with an additional matrix named \mathbf{K}^{NL} , in order to find optimal values for the system. Under the aid of a Fourier transform, the system can be formulated in the frequency domain as,

$$(-\omega^2 \mathbf{M} + i\omega \mathbf{C} + \mathbf{K} + \mathbf{K}^{NL})\mathbf{u}_f(\omega) = \mathbf{M}\mathbf{I}u_g(\omega) \quad (7)$$

where \mathbf{I} represents the identity vector, while $u_g(\omega)$ denotes the ground motion spectrum and $\mathbf{u}_f(\omega)$ is the response spectrum of the structure. From this expression, the transmission matrix can be obtained as,

$$\mathbf{H}(\omega, \mathbf{X}^{NL}) = [-\omega^2 \mathbf{M} + i\omega \mathbf{C} + \mathbf{K} + \mathbf{K}^{NL}]^{-1} \quad (8)$$

This linearized transmission matrix will be obtained for the wire rope setup and the NSE setup, and subsequently parameterized on the parameter vector \mathbf{X}^{NL} , which contains the system properties of interest. The Power Spectral Density (PSD) of the response can then be obtained with,

$$\mathbf{S}_u(\omega, \mathbf{X}^{NL}) = |\mathbf{H}(\omega, \mathbf{X}^{NL})|^2 \mathbf{S}_{\ddot{u}_g}(\omega) \quad (9)$$

Where, $\mathbf{S}_u(\omega, \mathbf{X}^{NL})$ is the PSD of the response, and $\mathbf{S}_{\ddot{u}_g}(\omega)$ is the PSD of the ground motion Eq. (5). According to the transformation by Wiener-Khinchine [12] the variance of a signal can be obtained from the relationship between PSD and auto correlation function with,

$$\sigma^2 = R(0) = \int_{-\infty}^{+\infty} S_u(\omega) d\omega \quad (10)$$

With Eq. (10) the variance of the response can be evaluated for every degree of freedom (DOF) in the system and used to calculate the response of the impulsive mode as,

$$\sigma_{rel}^2 = \int_{-\infty}^{+\infty} S_i(\omega, \mathbf{X}^{NL}) - S_s(\omega, \mathbf{X}^{NL}) d\omega \quad (11)$$



where, $S_i(\omega, \mathbf{X}^{NL})$ represents the variance of the impulsive mode, while $S_s(\omega, \mathbf{X}^{NL})$ is the variance of the top slab relative to the ground motion. The performance of the system can now be calculated with the following index,

$$PI(\mathbf{X}^{NL}) = \frac{\sigma_{META}^2(\mathbf{X}^{NL})}{\sigma_{TRAD}^2} \quad (12)$$

Where, PI stands for Performance Index, while $\sigma_{META}^2(\mathbf{X}^{NL})$ is the response of the impulsive tank mode when protected via the Metafoundation; whereas σ_{TRAD}^2 denotes same response when situated on a concrete slab. Note that the system performance improves when $PI < 1$.

3.1 Transmission matrix for the wire rope setup

In order to obtain the linearized transmission matrix of the wire rope setup, an SLT is employed. The SLT is a relatively straightforward tool to define an equivalent linear system through equating its stochastic response to the response of the nonlinear system. More precisely, the nonlinear differential equation (3) becomes,

$$\dot{z} + c_{eq}\dot{u} + k_{eq}z = 0 \quad (13)$$

where c_{eq} and k_{eq} are linearization coefficients that are ‘‘equivalent’’ in a statistical sense. SLT gives the expression of $z(t)$ to be substituted in the EOM, which can be rewritten as

$$-\omega^2 u_0 e^{i\omega t} m + i\omega u_0 e^{i\omega t} c + \alpha u_0 e^{i\omega t} k - \frac{i\omega}{i\omega + k_{eq}} c_{eq} (1 - \alpha) k u_y u_0 e^{i\omega t} = F_0 e^{i\omega t} \quad (14)$$

It is now possible to define the transfer function $H(\omega)$ and subsequently the transmission matrix for a multi degree of freedom system in the nonlinear case as follows,

$$H(\omega) = \left[-\omega^2 m + i\omega c + \alpha k - \frac{i\omega}{i\omega + k_{eq}} c_{eq} (1 - \alpha) k u_y \right]^{-1} \quad (15)$$

$$\mathbf{H}(\omega) = \left[-\omega^2 \mathbf{M} + i\omega \mathbf{C} + \mathbf{K}^L - \frac{i\omega}{i\omega + k_{eq}^{n,k}} c_{eq}^{n,k} u_y \mathbf{K}^{NL} \right]^{-1} \quad (16)$$

where $c_{eq}^{n,k}$ and $k_{eq}^{n,k}$ are linearization coefficients of the n -th resonator in the k -th layer. For the optimization procedure in the nonlinear case the design variables $k_{n,k}$, $A_{k,n}$, $\beta_{k,n}$ and $\gamma_{k,n}$ are collected in the parameter vector \mathbf{X}^{NL} and the optimization problem is stated as follows,

$$\min_{k,n} PI_{dr}(\mathbf{X}^{NL}) \quad \text{and} \quad \min_{k,n} PI_{acc}(\mathbf{X}^{NL}) \quad (17)$$

subjected to constraints and bounds on the design variables.

$$\beta_{k,n} + \gamma_{k,n} = 1 \quad (18)$$

$$A_{k,n} = 1 \quad (19)$$

$$0 < \beta_{k,n} < 1 \quad \text{and} \quad 0 < \gamma_{k,n} < 1 \quad (20)$$

4. Choice of hysteretic damper, Bouc-Wen parameters and optimization results

Paolacci and Giannini [7] characterized a set of wire ropes through experimental tests and found a good correspondence between the behavior of the Bouc-Wen model and the investigated wire ropes. Out of the wire ropes they analyzed, the one with the highest load capacity is the WR36-400-08 produced by the company ENIDINE. The geometric dimensions of the considered wire ropes are collected in Table 4, in which k_h and



F_v represent the horizontal stiffness and the vertical load capacity, respectively. [7] found $\alpha = 0.254$ and $u_y = 2.2\text{mm}$. Fig. 6b also shows typical behavior of a steel wire rope subjected to shear forces.

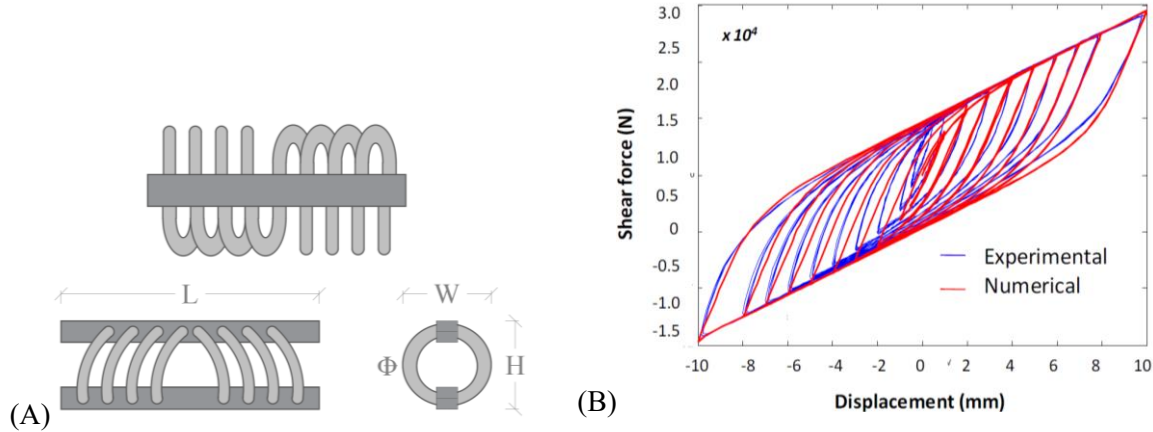


Fig. 3 - (A) Details of wire ropes and (B) shear cycles

Table 2. Geometric and mechanical characteristics of wire ropes.

Geometric characteristics				Parameters of Bouc-Wen model					
H	W	L	Φ	k_h	F_v	u_y	n	A	α
[mm]	[mm]	[mm]	[mm]	[kN/mm]	[kN]	[mm]			
178	216	520.7	26.6	1.35	2.97	2.2	1.0	1.0	0.254

4.1 Optimization results and comparison with time history analyses in the non-linear regime

When computing the optimal values for the parameters collected in \mathbf{X}^{NL} , optimization surfaces for one layered and two layered systems can be plotted as depicted in Fig. 4, where k_2 represents the post-yielding stiffness of the Bouc-Wen model. Clearly an optimal value for the stiffness of the wire ropes can be found, while the hysteresis parameters have only a minor impact on the performance index PI. Furthermore, it can be seen that the two layered case performs worse than the one layered case, with a PI greater than 1. From these values, the optimal number of WR36-400-08 wire ropes can be estimated to be 42 and 30 for the bottom and top side of the resonators, respectively. Clearly, these values are excessive for one resonator and a different type of wire rope needs to be selected. Due to the lack of experimental data on the hysteretic behavior of other wire ropes, an ideal wire rope endowed with the optimal parameters was used for the simulations in the time domain. Note that finding a wire rope exerting these properties is a technological issue and therefore not within the scope of this work.

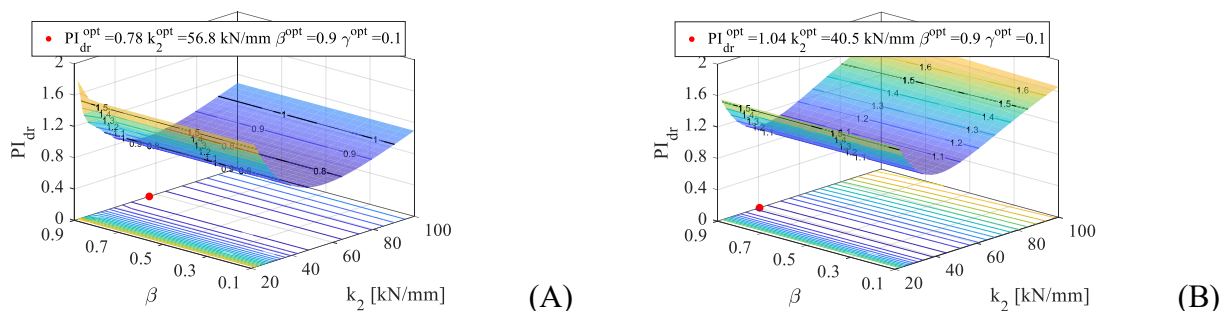


Fig. 4 - Wide parametric study: (A) optimization surface for one layered CMS and (B) two-layered CMS.

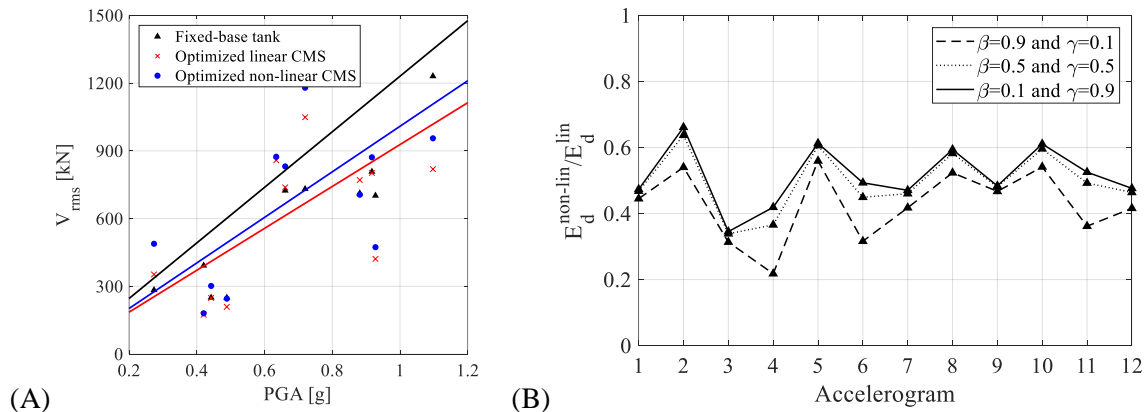


Fig. 5 - Results of the THAs: (A) Root mean square values of the base shear of one-layered system for $\beta = 0.9$ and $\gamma = 0.1$; (B) Ratio of the dissipated energy by linear and non-linear systems for the considered optimal configurations for one-layered case.

In the interest of brevity, only the results for the one layered case are shown in Fig. 5. Here, the response of the nonlinear system is compared to a system with linear visco-elastic dampers and a system with a fixed base. As can be seen from Fig. 5 (A), the linear system performs slightly better than the nonlinear system, due to the capability of the dampers to dissipate energy. Besides this, Fig. 5 (B) compares the dissipated energy of various setups with different hysteresis parameters, and shows that the hysteretic wire ropes are not able to reproduce the excellent damping values of visco-elastic dampers. However, it is worth mentioning that wire ropes represent a cheap and easily realizable solution that aids the feasibility of the Metafoundation.

5. Description of the structure endowed with negative stiffness components

In order to reduce the size of the foundation, NSEs are implemented to amplify the resonator motion. In Fig. the NSE is displayed with its components (A), its representation as a dynamic system (B), and its force equilibrium in the displaced state (C). On the other hand, Fig. 7 (A) shows the side view of the foundation with the NSEs inside, while Fig. (B) depicts the layout and the number of resonators, whereas Fig. (C) shows the cross section of one column. Note that for this layout the height of the foundation, the height of the resonators, and the width of the column cross section, are parameterized with h_F , h_R , and t_c , respectively, and vary for each investigated setup. The FULL, and MINIMAL systems were designed equivalently to the wire rope setup, which resulted in the values displayed in Table 3.

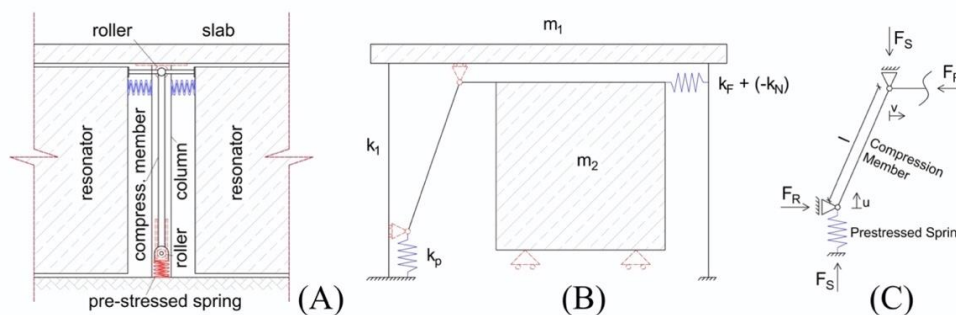


Fig. 6 – Negative Stiffness Mechanism NSE: (A) Component view; (B) Dynamic system; (C) Force equilibrium on the displaced system.

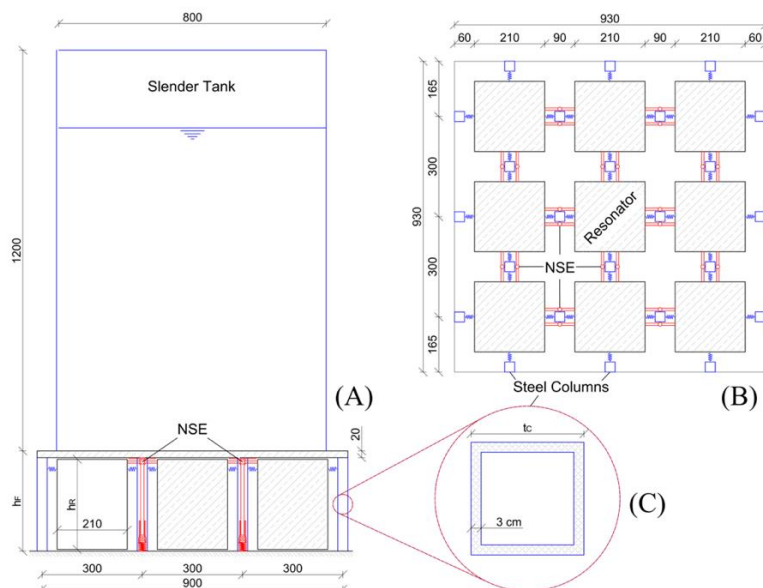


Fig. 7 – Schematics of the Metafoundation: (A) Side view; (B) Layout of the resonators and columns; (C) Cross section of a steel column (dimensions in cm) [12].

The idea behind the mechanism is to prestress a compression member and guide its movement along the column and the top slab of the foundation. When the system is excited horizontally, the resonators will displace, and subsequently incline the compression member, which then releases the potential energy stored in the prestressed spring onto the resonators. The force pair F_R acts on the one end of the compression member on the resonator, and on the other end on the column of the foundation. This force pair is dependent on the relative displacement between resonator and bottom slab and can therefore be regarded as a spring with a negative and nonlinear force displacement relationship. Furthermore, the dynamic system of the overall foundation is displayed in Fig. 6, where m_1 denotes the mass of the concrete slab; k_i , m_i , k_c , and m_c , represent the stiffness and mass of the tanks impulsive and convective mode, respectively; while k_R and c_R are the stiffness and damping ratio of the resonators. Note that k_R is in fact a compound stiffness comprised of k_F and $-k_N$, where k_F is responsible for the resonant frequency, while $-k_N$ counteracts the negative force deriving from the NSE. More particular, k_N represents the linear value of the negative stiffness for the undisplaced system (this will be elaborated in a later section), which has the following two advantages: (i) if k_F tends towards 0 the stability of the resonator is still fulfilled, since the negative stiffness deriving from the NSE is counteracted by $-k_N$; and (ii) since the negative stiffness of the NSE is counteracted by $-k_N$, k_F governs the frequency of the resonator with $\omega_R = \sqrt{k_F/m_2}$. The relevant parameters are summarized in Table 4 for the FULL, and MINIMAL system, respectively.

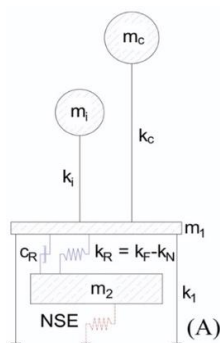


Fig. 6 – Dynamic system of the foundation including a fuel storage tank and the NSE.



Table 3. Geometric properties of the various foundation setups

Parameter	FULL	MINIMAL
h_F [cm]	300	100
h_R [cm]	270	75
t_C [cm]	30	17
l [cm]	270	70

Table 4. Parameters for the discretized system.

Parameter	FULL System	MINIMAL System
m_1 [kg]	5.88358e+04	4.36692e+04
m_2 [kg]	2.67907e+05	7.93800e+04
k_l [N/m]	8.50176e+08	3.30624e+09

5.1 Negative Stiffness Element NSE

In Fig. (C) F_R is the horizontal force deriving from the mechanism, which needs to be put in relation to the relative displacement v between bottom slab and resonator. Furthermore, F_S denotes the vertical force applied to the prestressed spring deriving from the mechanism, while l is the length of the compression member, and u describes the vertical displacement of the compression member's bottom end. The following relations can be drawn from Fig. (C),

$$F_S(u) = u \cdot k_p - P \quad (21)$$

$$F_R(v) = \frac{F_S}{(l-u)/l} \cdot \frac{v}{l} \quad (22)$$

$$(l-u)^2 = l^2 - v^2 \quad (23)$$

where k_p quantifies the stiffness of the prestressed spring, while P is the total amount of prestress applied to the system when in the vertical rest position. From these expressions, the nonlinear force displacement relationship of F_R can be obtained as,

$$F_R(v) = \frac{v(-P + k_p(l - \sqrt{l^2 - v^2}))}{\sqrt{l^2 - v^2}} \quad (24)$$

This expression can only be solved with nonlinear time integration, since a displacement of $v \rightarrow l$ entails an infinite stiffness. Therefore, an approximation was desired and estimated with a 3rd order Taylor polynomial at the origin,

$$F_{RT}(v) = -\frac{P}{l}v + \frac{k_p l - P}{2 l^3}v^3 + HO(v^5) \quad (25)$$

This expression shows a negative linear stiffness and a nonlinear positive stiffening effect characterized by,

$$F_{RT}(v) = a_{NSE}v + b_{NSE}v^3, \quad a_{NSE} = -\frac{P}{l} = k_N, \quad b_{NSE} = \frac{k_p l - P}{2 l^3} = \frac{k_p}{2 l^2} \left(1 - \frac{P}{k_p l}\right) \quad (26)$$

From these equations it can be deduced that the maximal negative stiffness appears at the origin with $k_N = a_{NSE} = -P/l$. This stiffness will be used as a linear approximation for the NSE during optimization and in the compound stiffness $k_R = k_F - k_N$. Furthermore, the stiffness of the prestressed spring k_p appears only in the nonlinear element of the approximation and can therefore be used to tune the nonlinearity. More precisely, a dimensionless nonlinearity parameter can be established with,

$$\epsilon = 1 - \frac{P}{k_p l}, \quad 0 \leq \epsilon \leq 1 \quad (27)$$

If ϵ becomes 0, the system behaves linear, while a value of $\epsilon = 1$ entails strong nonlinearity. Note that from this parameter, k_p can be obtained once the desired initial prestress P and compression member length l are defined. For the setups under study, $\epsilon = 0.95$ was regarded as a realistic value for all systems.



5.2 Stability condition

The NSE applies an amplification force on the resonator and thereby improves the system performance. This has a limit however, since the local instability can cause a global instability, if the negative stiffness exceeds a certain value. In the interest of brevity, the derivation of this limit is omitted herein, while only the governing stability limit is presented with,

$$k_N > \frac{k_F}{2} - \sqrt{\frac{k_F^2}{4} + k_1 k_F} \quad (28)$$

The minimum value obtained from Eq. (28) determines the maximum negative stiffness $k_{N\max}$, to which all further calculations refer in percent %.

5.3 Transmission matrix of the NSE system

For the optimization procedure proposed in Eqs. (6)-(12), the transmission matrix of the system needs to be written in its linear form. In order to obtain this, we start with the nonlinear EOMs,

$$M\ddot{u}(t) + C\dot{u}(t) + Ku(t) + F_{RT}(t) = F(t) \quad (29)$$

where $F_{RT}(t)$ represents the nonlinear relationship of the NSE as expressed in Eq. (24). Conveniently, this can be linearized by substituting the expression with Eq. (25) and setting $\epsilon = 0$. This system can now be optimized analogously to the wire rope setup (see Eq. (17)) with the parameter vector $X^{NL} = (k_F, c_R, k_N)$, containing the frequency, damping, and negative stiffness value of the system.

6. Optimization results and comparison with time history analyses

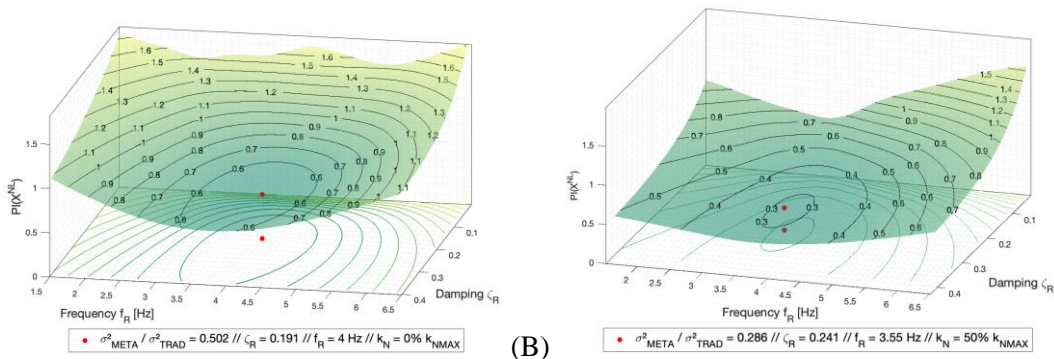


Fig. 7 – Optimization surface plots for: (A) FULL system with 25% NSE; and (B) FULL system with 75% NSE.

Fig. 7 shows the optimization plots for the FULL system with 25%, and 75%, of the maximum NSE value, respectively. Note that the PI improves for an increase in NSE, and that the overall shape of the plot becomes flatter, making the system less sensitive to frequency changes. This procedure was applied to the FULL, and MINIMAL systems, with the optimal damping and frequency, ζ_R and f_R , of the resonators being summarized in Table 5.

Table 5. Results from the optimization.

NSE % of $k_{N\max}$	FULL			MINIMAL		
	f_R [Hz]	ζ_R [-]	PI [-]	f_R [Hz]	ζ_R [-]	PI [-]
0	4.00	0.19	0.502	5.85	0.03	0.882
50	3.55	0.24	0.286	6.10	0.06	0.617



With optimal values obtained from the optimization procedure, the complete dynamic system can be constructed. Note that the length of the compression member l was chosen to fit inside the foundation, while the prestress force P subsequently resulted from Eq. (26). With these system parameters fixed, k_p was then evaluated from Eq. (27) with $\epsilon = 0.95$. The maximal base shear values for the investigated seismic records are displayed in Fig. 8 and show how the performance improves with an increase in negative stiffness. Furthermore, when observing the results for the FULL system without the NSE and the MINIMAL system at 50% of the maximum NSE value, it can be seen that the performance is virtually the same. Besides this the flattening of the lines with higher NSE levels show that the foundation performs more reliably under the aid of negative stiffness.

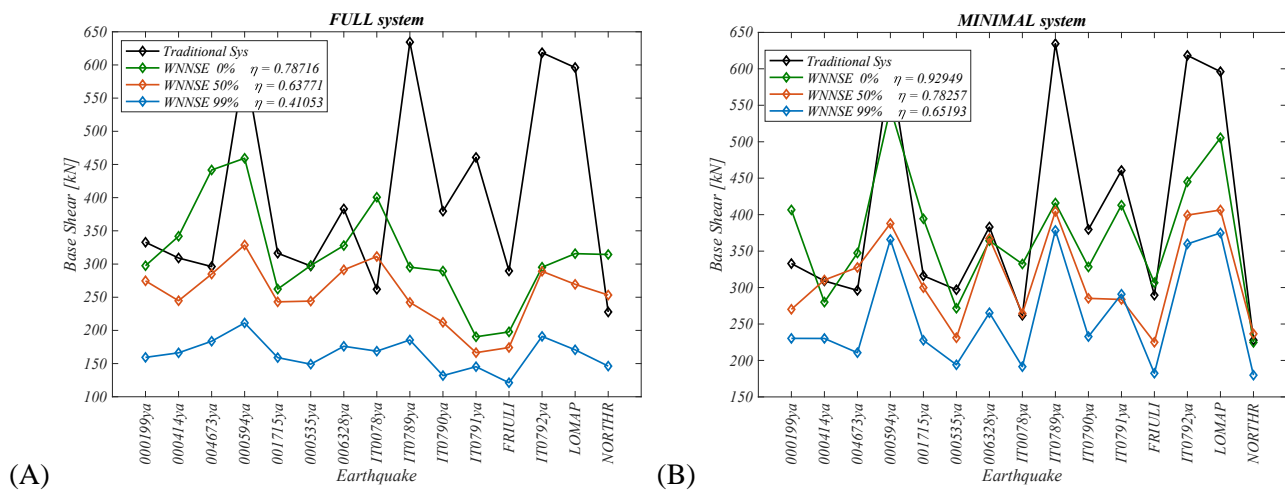


Fig. 8 – Time history results for: (A) FULL system; and (B) MINIMAL system.

7. Conclusion

In this paper, we proposed two metafoundations designed to inherit favorable properties from seismic wave propagating in phononic structures in the ultralow-frequency regime: i) a foundation equipped with nonlinear hysteretic dampers; and ii) a foundation equipped with negative stiffness devices. They both are composed by steel-concrete composite and steel components that define unit cells that contain resonating concrete masses. The tuning of this coupled systems was achieved through an optimization procedure in the frequency domain, which is able to account for the superstructure as well as the stochastic nature of the seismic input. In particular, to optimize the non-linear behavior of damper devices we employed a Bouc-Wen hysteretic model and to reduce the non-linear differential equations of Bouc-Wen models to a system of linear equations, we adopted the stochastic linearization technique. Then, we tested the optimized systems against natural seismic records with nonlinear time history analyses. A novel type of NSE was adopted for the application to a metamaterial-based foundation system. The mechanism contains a prestressed compression member held in a stable snap through position and is effectively able to improve the system performance. Due to the local instability, an inevitable nonlinearity is present in the system, which has been taken into account. By means of a Taylor series approximation, the force displacement relationship was simplified, and the nonlinearity parameter ϵ deduced. With this parameter the mechanism properties can be chosen according to the nonlinear behavior, while the ideal system can be reduced to a linear one with $\epsilon = 0$. Furthermore, an optimization procedure based on linear computations in the frequency domain was proposed herein, which takes the ground motion as well as the superstructure into account. The obtained optimal values were then used to construct fully nonlinear dynamic systems, which were subsequently investigated on their performance during realistic ground motions.

In particular, the optimization of the foundation equipped with hysteretic devices showed that excellent results could be achieved with simple dampers endowed with high dissipative characteristics, like the case of wire ropes, for a foundation as much as possible flexible. These results lay down the basis for future



developments of the Metafoundations where a proper use of nonlinear hysteretic devices or nonlinear mechanisms, like impact, can enhance the performance of finite lattice phononic structures. With regard to the use of NSE, the results showed that with only 50% of the maximum NSE value, the system could be reduced from 3 m to 1 m, while maintaining its performance level. Moreover, the NSE endowed system also increased its reliability across multiple ground motions. In sum, the proposed mechanism can significantly improve the functionality of a metamaterial-based system and may also be used for other vibration attenuation issues, such as the isolation of sensitive laboratory equipment.

8. Acknowledgements

The first author acknowledges funding from the Italian Ministry of Education, University and Research (MIUR) in the frame of the "Departments of Excellence" grant L. 232/2016 and the SERA grant agreement no. 730900. Furthermore, this project has also received funding from the European Union's Horizon 2020 research and innovation program under the Marie Skłodowska-Curie grant agreement no. 721816 for the second author.

9. References

- [1] A. Barka, "The 17 August 1999 Izmit earthquake," *Science* (80-.), vol. 285, no. 5435, pp. 1858–1859, Sep. 1999.
- [2] E. Krausmann, E. Renni, M. Campedel, and V. Cozzani, "Industrial accidents triggered by earthquakes, floods and lightning: Lessons learned from a database analysis," *Nat. Hazards*, vol. 59, no. 1, pp. 285–300, Oct. 2011.
- [3] J. M. Kelly and D. A. Konstantinidis, *Mechanics of Rubber Bearings for Seismic and Vibration Isolation*. John Wiley and Sons, 2011.
- [4] V. A. Zayas, S. S. Low, and S. A. Mahin, "A Simple Pendulum Technique for Achieving Seismic Isolation," *Earthq. Spectra*, vol. 6, no. 2, pp. 317–333, May 1990.
- [5] M. Wenzel, F. Basone, and O. S. Bursi, "Design of a Metamaterial-Based Foundation for Fuel Storage Tanks and Experimental Evaluation of Its Effect on a Connected Pipeline System," *J. Press. Vessel Technol. Trans. ASME*, 2020.
- [6] F. Basone, M. Wenzel, O. S. Bursi, and M. Fossetti, "Finite locally resonant Metafoundations for the seismic protection of fuel storage tanks," *Earthq. Eng. Struct. Dyn.*, vol. 48, no. 2, 2019.
- [7] F. Paolacci and R. Giannini, "Study of the Effectiveness of Steel Cable Dampers for the Seismic Protections of Electrical Equipment," in *World Conference in Earthquake Engineering*, 2008.
- [8] V. La Salandra, M. Wenzel, O. S. Bursi, G. Carta, and A. B. Movchan, "Conception of a 3D metamaterial-based foundation for static and seismic protection of fuel storage tanks," *Front. Mater.*, vol. 4, Oct. 2017.
- [9] P. K. Malhotra, T. Wenk, and M. Wieland, "Simple procedure for seismic analysis of liquid-storage tanks," *Struct. Eng. Int. J. Int. Assoc. Bridg. Struct. Eng.*, vol. 10, no. 3, pp. 197–201, 2000.
- [10] Caughey TK (1963) Equivalent Linearization Techniques. *Journal of the Acoustical Society of America*, Vol. 35, No11, pp. 1706-1711
- [11] A. Bonelli and O. S. Bursi, "Generalized- α methods for seismic structural testing," *Earthq. Eng. Struct. Dyn.*, vol. 33, no. 10, pp. 1067–1102, Aug. 2004.
- [12] R. W. Clough and J. Penzien, *Dynamics of structures*. McGraw-Hill, 1975.
- [13] M. Wenzel, O. S. Bursi, and I. A. Antoniadis, "Optimal finite locally resonant metafoundations enhanced with nonlinear negative stiffness elements for seismic protection," *J. Sound Vib. under Rev.*, 2019.